

G_{ep}/G_{mp} via Simultaneous Asymmetry Measurements
of the Reaction $\vec{p}(\vec{e}, e')$

May 31, 2001

J. Jourdan, D. Rohe, I. Sick, G. Warren*
University of Basel, Basel, Switzerland

R. Ent, D. Mack
Jefferson Lab, Newport News, VA

A. Klein
Old Dominion University, Norfolk, VA

B. Zihlmann
Vrije University, Amsterdam, The Netherlands

D. Crabb, D. Day, P. McKee, O. Rondon, F. Wesselmann, M. Zeier, H. Zhu
University of Virginia, Charlottesville, VA

* Spokesperson

Abstract

Recent polarization transfer experiments in Hall A have shown that the ratio of the proton electric and magnetic form factors $\mu_p G_{ep}/G_{mp}$ significantly departs from unity as Q^2 increases. This result disagrees with earlier Rosenbluth separation measurements. We propose to measure this ratio via simultaneous measurements of the beam-target asymmetry for the reaction $\vec{p}(\vec{e}, e')$ at $Q^2 = 1.10$ and 2.10 GeV^2/c^2 with 2% systematic errors and 3% statistical errors. The advantage of the simultaneous asymmetry measurements is that the leading systematic uncertainties from the polarized target vanish to first order.

1 Introduction

A precise understanding of the electromagnetic form factors of the proton is of vital interest to both the nuclear and particle physics communities. The momentum dependence of the form factors of the proton G_{ep} and G_{mp} are a consequence of the charge and current distribution of the proton. Knowledge of this structure may lead to a better understanding of the constituents of the proton and how they interact. Likewise, a thorough understanding of this structure is one of the necessary ingredients to understand the dynamics of hadrons in the nuclear medium.

Earlier experiments [1, 2, 3, 4, 5, 6, 7], which were based on the Rosenbluth separation technique[8], showed that both G_{ep} and G_{mp} roughly follow the dipole parameterization. This observation was strengthened by two global fits to the separation data [1, 2]. The similarity of the Q^2 dependence of G_{ep} and G_{mp} suggested that both the charge and the current structure of the proton are the same.

Results from a series of measurements performed in Hall A have seriously questioned the earlier experimental results [9]. These experiments measured polarization transfer in the elastic scattering of polarized electrons from protons. By taking the ratio of the polarization transfer components P_L and P_T , they extracted the ratio

$$g \equiv \mu_p G_{ep}/G_{mp}, \tag{1}$$

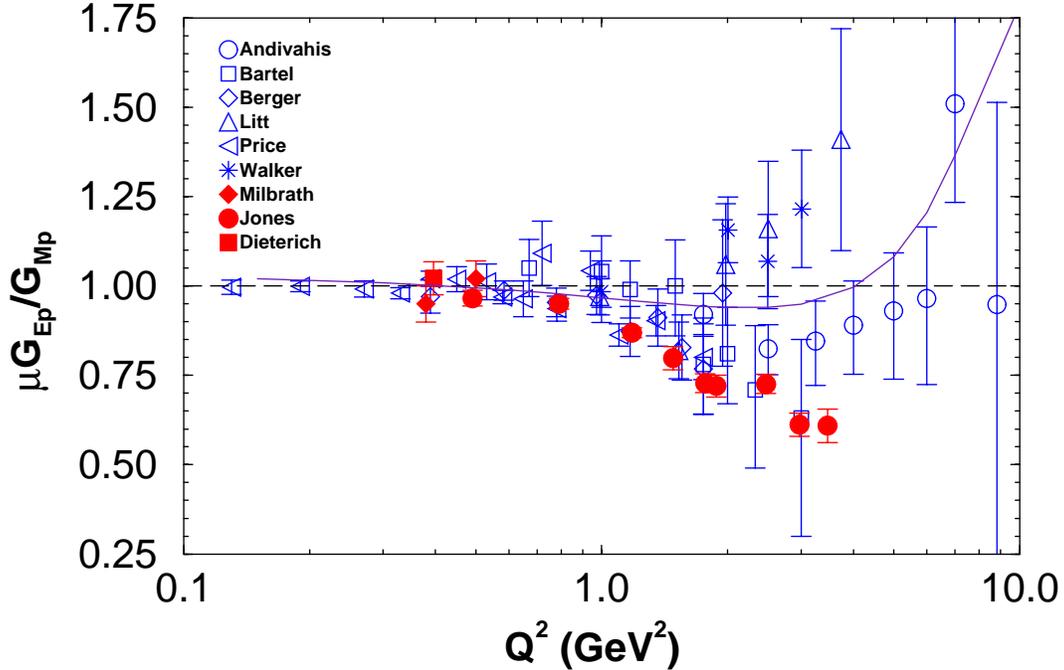


Figure 1: World's Data for $\mu_p G_{ep}/G_{mp}$. The solid red points are proton polarimetry measurements. The other points are extracted from cross section measurements. The solid curve is a quadratic fit to the global analysis of the L/T data of Walker *et al.*.

with small systematic uncertainties compared to the earlier Rosenbluth separation measurements. Their results show that g significantly departs from 1.0 for $Q^2 > 0.5 \text{ GeV}^2/c^2$, as seen in Fig 1. As a consequence of the Hall A results, one must conclude that the charge and the current distribution in the protons are significantly different. We are left with an uncomfortable situation: two distinct measurements have yielded two results with radically different physical interpretations.

We have examined ways to measure G_{ep}/G_{mp} using the UVa NH_3 target as a polarized proton target. The leading systematic uncertainties for a single asymmetry measurement are due to the dilution factor and the target polarization. In the past, these errors have at best been determined to 4% and 3%, respectively. One may be able to do moderately better through careful systematic studies, but the uncertainties are unlikely to fall below 3.5% and 2.5%. For this reason, we studied the possibility of conducting a simultaneous double asymmetry measurement. By taking the ratio of simultaneously measured asymmetries, we

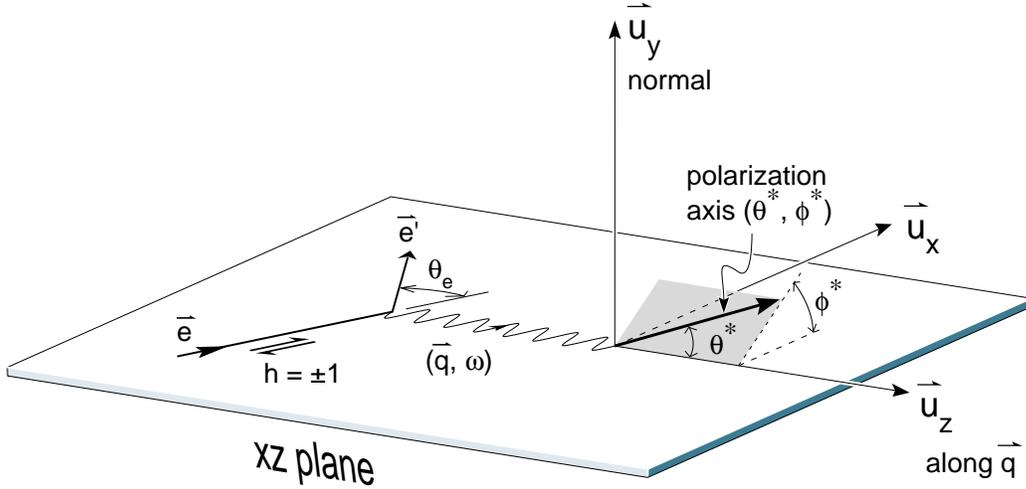


Figure 2: Coordinate system for $\vec{p}(\vec{e}, e')$ with orientation of polarization axis.

can eliminate the uncertainties in the dilution factors and target polarization to first order. In this manner, we can conduct a highly accurate measurement of G_{ep}/G_{mp} in the same range as the Hall A measurements.

2 Method

Following Donnelly and Raskin [10], we can express the inclusive $e - p$ cross section as a sum of an unpolarized part Σ , that corresponds to the elastic cross section $d\sigma/d\Omega_e$, and a polarized part Δ that is different from zero only when the beam is longitudinally polarized (helicity h):

$$\sigma(h) = \Sigma + h\Delta; \quad h = \pm P_b, \quad (2)$$

where P_b is the polarization of the electron beam. The beam-target asymmetry is

$$A = \frac{\sigma_+ - \sigma_-}{\sigma_+ + \sigma_-} = \frac{\Delta}{\Sigma}. \quad (3)$$

The elastic unpolarized free $e - p$ cross section is

$$\Sigma(E, \theta) = \sigma_{mott} \frac{E'}{E} \left\{ \frac{1}{1 + \tau} G_{ep}^2 + \left[\frac{\tau}{1 + \tau} + 2\tau \tan^2(\theta/2) \right] G_{mp}^2 \right\}, \quad (4)$$

where $E(E')$ is the electron's initial (final) energy, θ is the electron's scattering angle, $\tau = Q^2/4m_p^2$, m_p is the mass of the proton, $Q^2 > 0$ is the four-momentum transfer

squared, and G_{ep} and G_{mp} are the proton electric and magnetic form factors.¹ The polarized part Δ contains two terms controlled by the orientation of the target polarization. The full expression is given below, with the kinematic factors and the nucleon form factors evaluated in the lab frame:

$$\begin{aligned} \Delta(E, \theta, \theta^*, \phi^*) &= -2\sigma_{mott} \frac{E'}{E} \sqrt{\frac{\tau}{1+\tau}} \tan(\theta/2) \\ &\times \left\{ \sqrt{\tau(1+(1+\tau)\tan^2(\theta/2))} \cos\theta^* G_{mp}^2 + \cos\phi^* \sin\theta^* G_{ep} G_{mp} \right\}, \end{aligned} \quad (5)$$

where θ^* and ϕ^* are the laboratory angles of the target polarization vector with \vec{q} along \hat{u}_z and \hat{u}_y normal to the scattering plane, see Fig 2. The experimental asymmetry ϵ is related to A by

$$\epsilon = P_b P_t f A(E, \theta, \theta^*, \phi^*), \quad (6)$$

where P_t is the target polarization and f is the dilution factor.

We propose to conduct double beam-target asymmetry measurements in which the two spectrometers are located on either side of the beam with equal scattering angles. We can then form the ratio of the two measured asymmetries

$$R = \frac{f_1 \Delta(E, \theta_1, \theta_1^*, \phi_1^*) \Sigma(E, \theta_1)}{f_2 \Delta(E, \theta_2, \theta_2^*, \phi_2^*) \Sigma(E, \theta_2)}, \quad (7)$$

where $\theta_i, \theta_i^*, \phi_i^*$ are the scattering angle and target polarization angles for the i^{th} spectrometer. It is conceivable that with two different spectrometers, the dilution factors will be slightly different. For this reason, we retain the ratio of the dilution factors. The target and beam polarizations, however, cancel. This eliminates one of the larger systematic uncertainties of a single beam-target asymmetry measurement.

So that the beam-target asymmetry is sampling the same Q^2 in both electron arms, the scattering angles of both spectrometers must be equal. Otherwise, we would be comparing form factors for different Q^2 in the numerator and denominator of R . We refer to the assumption of $\theta_1 = \theta_2$ as the linearity assumption, because with this assumption, the numerator and denominator of Eqn. 7 are linear in G_{ep} :

$$R = \frac{f_1 a(E, \theta_1) \cos\theta_1^* G_{mp}^2 + \sin\theta_1^* \cos\phi_1^* G_{mp} G_{ep}}{f_2 a(E, \theta_2) \cos\theta_2^* G_{mp}^2 + \sin\theta_2^* \cos\phi_2^* G_{mp} G_{ep}}, \quad (8)$$

¹Note that we have chosen to express the elastic kinematics in terms of E and θ throughout this document.

where

$$a(E, \theta) = \sqrt{\tau(1 + (1 + \tau) \tan^2(\theta/2))}. \quad (9)$$

For compactness of notation, we have omitted that E' and τ depend on E and θ . We discuss the uncertainties in our results due to the linearity assumption in section 4.3.

We have retained the subscripts for the scattering angles in Eqn. 8, e.g. θ_1 and θ_2 , for completeness. While the spectrometers may be oriented so that the central rays into each spectrometer correspond to exactly equal scattering angles, the acceptance averaged scattering angles will in general not be identical. So it is important that these two angles be unique.

Ideally, one would set up an experiment in which $\theta_1^* = 90^\circ$ and $\theta_2^* = 0^\circ$ so that R is simply proportional to G_{ep}/G_{mp} . However, this configuration is not possible in general because of the occlusion of angles by the target magnet. One must then consider the more general case and invert Eqn 8:

$$g \equiv \mu_p \frac{G_{ep}}{G_{mp}} = -\mu_p \frac{a(\tau_1, \theta_1) \cos \theta_1^* - \frac{f_2}{f_1} R a(\tau_2, \theta_2) \cos \theta_2^*}{\cos \phi_1^* \sin(\theta_1^*) - \frac{f_2}{f_1} R \cos \phi_2^* \sin(\theta_2^*)} \quad (10)$$

In this manner, the ratio of the measured asymmetries R can be related to the ratio G_{ep}/G_{mp} .

3 Kinematics

Our approach is to optimize the experimental setup for the highest Q^2 measurement. For the lower Q^2 measurement, we hold the target field orientation and spectrometers fixed while reducing the beam energy by reducing the number of passes. Since the rates for the lower Q^2 data points are an order of magnitude higher, this approach minimizes our time on the floor of the experimental hall.

The selection of the highest Q^2 kinematics is driven by several considerations:

- It is preferred that the experiment be done in Hall C because of the existing infrastructure and experience with the target. This constrains the maximum scattering energy of the electrons to around 2 GeV because of the SOS. It is not necessary for the experiment to be performed with two identical spectrometers, merely with two spectrometers in which the acceptance averaged quantities after kinematic cuts are similar.

- The scattered electrons and beam must pass through the target magnet with adequate clearance.

The time to do the measurement is calculated assuming a given statistical error in g . An uncertainty in g can be related to an uncertainty in R by

$$\delta g = \left| \frac{\partial g}{\partial R} \right| \delta R. \quad (11)$$

The uncertainty in the ratio of the asymmetry measurements is given by

$$(\delta R)^2 = R^2 \left[\left(\frac{\delta \epsilon_1}{\epsilon_1} \right)^2 + \left(\frac{\delta \epsilon_2}{\epsilon_2} \right)^2 \right]. \quad (12)$$

We can write the relative statistical uncertainty of the measured asymmetry as

$$\left(\frac{\delta \epsilon}{\epsilon} \right)^2 = \frac{1}{(P_t P_b f A)^2} \frac{1}{N} = \frac{1}{(P_t P_b f A)^2} \frac{1}{r_{tot} t}, \quad (13)$$

where N_{tot} is the total number of counts from all sources (i.e. from H,N,He,Al), r_{tot} is the total count rate and t is the time of the measurement. The total rate is related to the rate on the proton by $r_{tot} = r_p/f$; the dilution factor only appears linearly in the relative uncertainty of the measured asymmetry. We can then solve for t in the above equation to get

$$t = \frac{1}{(P_t P_b)^2} \left(\frac{1}{f_1 r_p^1 A_1^2} + \frac{1}{f_2 r_p^2 A_2^2} \right) \frac{R^2}{(\delta g)^2} \left(\frac{\partial g}{\partial R} \right)^2, \quad (14)$$

where we have considered different rates and dilution factors in the two spectrometers.

We have used a realistic set of parameters to determine the times to statistics, see Table 1. The dilution factors were determined using MCEEP with the analysis tools developed for the polarized target G_{en} measurement which ran in 1998 (E93-026). The rates are also determined by MCEEP. We used the nominal setup and cuts as discussed in section 4.1. These rates include losses due to radiative processes and acceptance matching.

The occlusion of angles by the target magnet significantly restricts the possible kinematics. A list of geometry parameters used to identify kinematics in which the beam and scattered electrons pass through the magnet orifices with adequate clearance is given in Table 2. We checked that the beam as well as the electrons scattered over the the entire volume of the target cell into the horizontal angular acceptance of the spectrometers restricted by kinematics cuts pass through the target magnet with adequate clearance.

$Q^2(\text{GeV}^2/c^2)$	1.1		2.1	
Parameter	HMS	SOS	HMS	SOS
luminosity ($\text{cm}^{-2}\text{s}^{-1}$)	$1 \cdot 10^{35}$			
P_b	0.70			
P_t	0.80			
rates (Hz)	1.9	1.3	0.18	0.12
f	0.60	0.56	0.77	0.77
$\delta g/g$	3%		3%	

Table 1: Factors used in calculations of rates and time to perform measurements.

raster radius	1 cm
target length	3 cm
bore diameter	20 cm
split between coils	10 cm
bore angle	$\pm 49^\circ$
split angle	$\pm 17^\circ$

Table 2: Geometric parameters used to determine the clearance of electrons through the magnet.

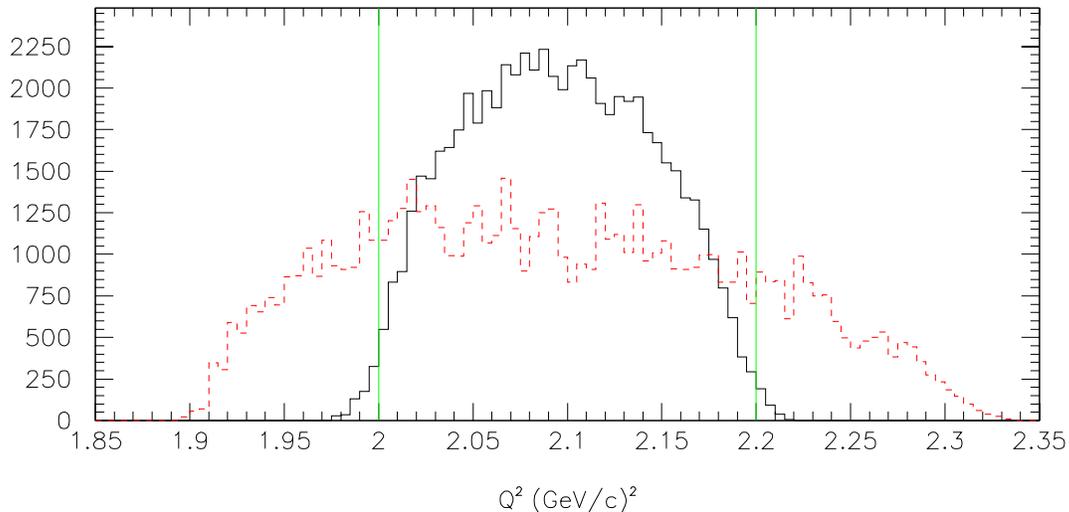


Figure 3: Overlap of acceptances for the HMS and SOS for the $Q^2=2.1$ point. The SOS is the dashed red histogram and the HMS is the solid black histogram. The green vertical lines indicate the Q^2 cut limits.

The target field deflection of the scattered electrons complicates the acceptance matching of the two spectrometers. Fortunately, we are interested in elastic scattering, which is confined to a small, well-defined region of the acceptance. The deflection does not significantly distort the acceptance for elastic events, but rather shifts it. This shift is compensated by offsetting the in-plane scattering angle of the two spectrometers so that the scattering angles are equal.

Figure 3 illustrates the overlap of the two spectrometers in Q^2 . The SOS and HMS have opposite collimator orientations: HMS is wide in the vertical angle and the SOS is wide in the horizontal angle. This difference results in the SOS Q^2 acceptance being wider than that of the HMS. Because of its vertical orientation, the HMS has a larger solid angle than the SOS over a given range of scattering angles. For this reason, we have oriented the target field so that the HMS detects the electrons with the smaller of the two asymmetries (the electrons roughly parallel to the target field). This orientation maximizes the figure of merit.

Some details of the experimental setup are given in Tables 3 and 4. The kinematic settings and the time to achieve 3% statistical uncertainty in g (assuming linear parameterization

Q^2 (GeV ² /c ²)	E (GeV)	E' (GeV)	θ_{HMS}^0 (°)	θ_{SOS}^0 (°)	θ_t (°)	time (h)
1.1	1.848	1.246	40.2	-39.5	-137.1	14
2.1	2.746	1.627	40.2	-39.5	-137.1	215

Table 3: Experimental Setup. θ^0 denotes the central horizontal angle of the spectrometers with respect to the beam, and not the scattering angle.

Q^2 (GeV ² /c ²)	HMS				SOS			
	θ^* (°)	ϕ^* (°)	θ_e (°)	A	θ^* (°)	ϕ^* (°)	θ_e (°)	A
1.10	94.4	177.7	40.2	0.32	166.3	96.7	40.2	0.53
2.10	102.2	177.9	40.1	0.34	167.3	57.5	40.1	0.62

Table 4: Acceptance averaged kinematic quantities as determined with MCEEP.

of the Hall A G_{ep}/G_{mp} results) are listed in the Table 3. The luminosity is calculated for 100 nA of beam current. Table 4 lists several acceptance averaged quantities as determined with MCEEP.

For the experimental setup, we will require several items typical for running with the UVa NH₃ target:

- a chicane to counter the effect of the target field on the beam,
- the slow raster to raster over the large target cell,
- the Basel Secondary Emissions Monitor to calibrate the absolute beam position,
- the Moller polarimeter to measure the beam polarization,
- various beamline instrumentation which are functional for the low current (100 nA) of this experiment.

4 Uncertainties

We examined several contributions to the systematic uncertainties of this experiment. They are:

- kinematic uncertainties,
- cut dependence,
- linearity assumption to go from Eqn. 7 to Eqn. 8,
- the ratio of the dilution factors,
- the contribution to the asymmetry from nitrogen.

To study most of these uncertainties, we used a version of MCEEP which included the target field. This version has been extensively tested for the E93-026 data analysis. While we did not consider tracking through the spectrometer itself, we did include resolution smearing of the reconstructed coordinates. The σ resolutions for the momentum, horizontal angle and vertical angle were 0.1%, 1 mrad and 1 mrad for the HMS and 0.1%, 3 mrad and 1 mrad for the SOS. We placed cuts on the invariant mass, $930 < W < 950$, and on the four-momentum transferred squared, $1.03 < Q^2 < 1.16$ and $2.0 < Q^2 < 2.2$ for the $Q^2 = 1.1$ and $2.1 \text{ GeV}^2/c^2$ respectively.

We have not included the effect of the extended target acceptances into our rate estimates. The HMS will certainly have no problem with the 3 cm long target. Because we are doing elastic scattering and we cut on Q^2 to match the HMS acceptance, the horizontal angular acceptance of the SOS is significantly restricted to a region where the extended target acceptance will be fairly flat.

4.1 Kinematical Uncertainties

We examined the effect of uncertainties in the kinematics on the extracted g . The calculation of the uncertainty is modestly complicated by the dependence of g and R on the kinematic variables. If we let χ be a general kinematic parameter (i.e. $\chi = \phi_e, \theta_e, \theta_t$ or E) which we

vary by $\pm\delta\chi$ and we denote values for the nominal setting with a subscripted zero, then the uncertainty in the extraction of g due to an uncertainty $\delta\chi$ in χ is given by

$$\delta g_\chi = \left| \frac{\partial g}{\partial \chi} \Big|_{R_0} \delta\chi + \frac{\partial g}{\partial R} \delta R \right|, \quad (15)$$

where

$$\frac{\partial g}{\partial \chi} \Big|_{R_0} \delta\chi = g(\chi_0, R_0) - g(\chi_0 + \delta\chi, R_0), \quad (16)$$

$$\frac{\partial g}{\partial R} \delta R = \frac{\partial g}{\partial R} \Big|_{\chi_0} (R_0 - R(\chi_0 + \delta\chi)), \quad (17)$$

$$R_0 = R(\chi_0), \quad (18)$$

$$(19)$$

where we have suppressed the dependencies of the variables held constant.

Using MCEEP, we studied the uncertainties in the extraction of g due to kinematical uncertainties. We varied one parameter at a time in MCEEP²; we varied the beam energy E by $\pm 0.1\%$, the central horizontal scattering angle ϕ by ± 1 mrad, the target field orientation θ_t by $\pm 0.1^\circ$, and the vertical deflection angle of the scattered electrons θ by $\pm 1\%$. The last variation is based on our knowledge of the target field integral to 1% or better. We took the larger of the two variations ($\pm\delta\chi$) for each parameter as the uncertainty due to that parameter. The results are shown Table 5.

4.2 Cut Dependence

We examined the effect of shifting the limits of the cuts on the extraction of g . The size of the shifts in W and Q^2 correspond to the uncertainties in those two quantities due to uncertainties in the beam energy and the scattering angle³. The shifts are ± 4 and ± 6 MeV in W and ± 0.008 and ± 0.012 GeV²/c² in Q^2 for $Q^2 = 1.1$ and 2.1 GeV²/c², respectively. The lower and upper limits were varied together. Adding the variations in g for variations in the cuts in W and Q^2 quadratically, we found that the extracted g varied by 0.30% and 0.48% for $Q^2 = 1.1$ and 2.1 GeV²/c², respectively.

²The two spectrometer angles were varied independently

³We are assuming the scattered electron energy is determined from the scattering angle.

	Kinematics		f_{HMS}/f_{SOS}		Linearity	
$Q^2(\text{GeV}^2/c^2)$	1.1	2.1	1.1	2.1	1.1	2.1
E	0.12%	0.15%	0.73%	0.98%	0.64%	0.63%
ϕ_{HMS}	0.28%	0.43%	0.19%	0.27%	0.75%	0.80%
ϕ_{SOS}	0.12%	0.08%	0.61%	0.51%	0.43%	0.27%
θ_{HMS}	0.06%	0.04%	0.13%	0.41%	0.17%	0.08%
θ_{SOS}	0.01%	0.01%	0.08%	0.14%	0.01%	0.03%
θ_t	0.47%	0.70%	n/a	n/a	0.14%	0.03%
total	0.58%	0.84%	0.98%	1.23%	1.10%	1.06%

Table 5: Uncertainties in the extracted g due to uncertainties in the kinematics, the ratio of dilution factors and the linearity assumption because of uncertainties in the kinematic parameters. See text for definition of parameters.

4.3 Linearity

When we extract g following Eqn 10, we have assumed that the averaged scattering angle measured with the two spectrometers is equal so that the ratio of the cross sections is exactly 1.0. Earlier we referred to this as the “linearity” assumption. This assumption is not generally true because the acceptance averaged quantities between the two spectrometers will not perfectly agree.

To determine the uncertainty due to the linearity assumption, we followed an approach similar to the one to determine the kinematic uncertainties, see Sec. 4.1. We tabulated the ratio of the cross sections for the HMS and SOS using the beam energy and the acceptance averaged scattering angle for the different kinematic perturbations. We found that the uncertainty in the ratio of the cross sections due to the uncertainties in the kinematic parameters to be 1.1% in g for both Q^2 points. The leading contributors were the beam energy uncertainty and the HMS in-plane scattering angle. A breakdown of the contributions to this uncertainty is shown in Table 5.

4.4 Dilution factors

The ratio of the dilution factors is less susceptible than a single dilution factor to uncertainties. A single dilution factor is sensitive at first order to the cross section, target material densities and spectrometer acceptance. However, the ratio of the dilution factors is sensitive only at second order to these quantities, because only the differences between the acceptances and resolutions of the two spectrometers may be significant.

Our approach to determining the uncertainty in the ratio of the dilution factors is similar to the approach to determine the kinematic uncertainties. We calculated the dilution factor for the perturbation in the kinematic parameters and determined the variation of these around the nominal setting. We found that the uncertainty in the ratio of the dilution factors was 1.0 and 1.2% for the $Q^2 = 1.1$ and $2.1 \text{ GeV}^2/c^2$ points, respectively. The leading contributors were the beam energy and the HMS angles. A breakdown of the contributions to this uncertainty is shown in Table 5.

4.5 Nitrogen Asymmetry

There are several materials in the target in addition to hydrogen; however, only nitrogen contributes to the asymmetry measurement. Although the asymmetry from nitrogen is less understood than that of the proton, nitrogen's contribution to the systematic uncertainty of this measurement is reduced by taking the ratio of asymmetries.

In a simple shell model picture of N^{15} , the only unpaired nucleon is the seventh proton in the $p_{1/2}$ shell. This is a reasonable first-order picture as N^{15} is just one hole in the double closed O^{16} nucleus. Indeed, the measured magnetic moment of N^{15} is very close to the Schmitt value, $-0.2832\mu_N$ compared to $-0.2643\mu_N$, so we have some confidence that this picture is correct at the 80% level. Thus, we expect the nitrogen asymmetry to be dominated by proton physics.

The polarization of the $p_{1/2}$ proton in N^{15} is reduced from the polarization of the free proton by several factors. First, the polarization of the nitrogen is only 1/6 that of the proton. Second, because of the combination of the angular momentums, the proton is anti-

aligned to the N^{15} spin a net one-third of the time.⁴ From this information, one expects that $A_N/A_p \approx 6\%$. The effect of this asymmetry is further reduced by the dilution factor: only about 30% of the events under the hydrogen elastic peak are due to nitrogen. At worst, the nitrogen contributes only about 2% of the observed single arm asymmetry.

By taking the ratio of the asymmetries, we further reduce uncertainties due to the nitrogen. The ratio of the measured asymmetry accounting for the nitrogen is

$$R = \frac{\epsilon_1}{\epsilon_2} = \frac{f_p^1 A_p^1 + f_N^1 A_N^1}{f_p^2 A_p^2 + f_N^2 A_N^2}, \quad (20)$$

where the f_p^i (f_N^i) is the dilution factor for proton (nitrogen) [$f_j = N_j/N_{tot}$] for the i^{th} measurement, and A_p^i (A_N^i) is the asymmetry for the proton (nitrogen) for the i^{th} measurement. Rewriting R to be the proton asymmetry ratio and a correction due to the nitrogen asymmetry, one gets

$$R = \frac{f_p^1}{f_p^2} \cdot \frac{A_p^1}{A_p^2} \cdot \frac{1 + \frac{f_N^1}{f_p^1} \cdot \frac{A_N^1}{A_p^1}}{1 + \frac{f_N^2}{f_p^2} \cdot \frac{A_N^2}{A_p^2}}. \quad (21)$$

The third fraction is the one that will introduce any additional uncertainties due to the nitrogen. If we assume that the nitrogen asymmetry is dominated by proton physics, then the nitrogen asymmetry will simply be proportional to the proton asymmetry for both kinematics. In addition, the ratio of the dilution factors should not be significantly different for the two asymmetry measurements. Thus, the correction due to the nitrogen asymmetry is small because the numerator and denominator in the correction are approximately equal. The uncertainties in the relative asymmetries are due to the shell model approximation (20%) and the nitrogen polarization (10%), so that the nitrogen to proton asymmetry is $A_N/A_p \approx 0.060 \pm 0.013$. If we assume that only hydrogen and nitrogen are in the target, we get a worst case estimate of the ratio of the nitrogen to proton dilution factor. With a 5% uncertainty in this ratio, we find that the corrections to g due to the nitrogen asymmetry are $(0.72 \pm 1.31)\%$ and $(0.00 \pm 0.55)\%$ for $Q^2 = 1.1$ and $2.1 \text{ GeV}^2/c^2$ using the dilution factors listed in Table 1.

A summary of the systematic uncertainties is given in Table 6. The dominant uncertainties are the relative dilution factors and linearity for the $Q^2 = 2.1 \text{ GeV}^2/c^2$ point. For the

⁴The magnetic moment of N^{15} is negative, so the asymmetry of N^{15} has the same sign as that of the proton.

$Q^2(\text{GeV}^2/c^2)$	1.1	2.1
Kinematics Uncertainties	0.6%	0.8%
Cut dependence	0.3%	0.5%
Linearity	1.1%	1.1%
Dilution factor	1.0%	1.2%
Nitrogen asymmetry	1,3%	0.6%
total	2.1%	2.0%

Table 6: Summary of systematic uncertainties in the determination of g .

lower Q^2 point, the smaller dilution factor makes the nitrogen asymmetry contribution the leading uncertainty. However, the total systematic uncertainty is well below the statistical uncertainty. We wish to emphasize that this systematic uncertainty is obtainable without any heroic effort or demanding assumptions; the method itself removes the sensitivities to most systematics effects leaving simply the physics.

5 Comparison to other Experiments

A comparison of this experiment to other completed and proposed experiments is summarized in Fig. 4. We have plotted our projected results along the linear fit to the Hall A results. Our uncertainties depend on the ratio of the form factors. If g remains closer to one, the statistical and systematic relative uncertainties will both be smaller.

The $Q^2=2.1 \text{ GeV}^2/c^2$ point is more than 8σ from the global fit to the L/T data, and the error is only 40% of the Hall A uncertainties. For Hall A, the systematic uncertainties in g are largest in this kinematic region because the extraction of g is very sensitive to the precession of the protons' spin through the spectrometer. In comparison to the projected results for E01-001 [11], our uncertainties are considerably smaller. Another significant difference between our approach and the others is that we are statistics limited while they are systematics limited. Both the Hall A experiment and E01-001 will extract g for $Q^2 \sim 5 \text{ GeV}^2/c^2$. However, since the primary goal of this experiment is the separation of the Hall A and the

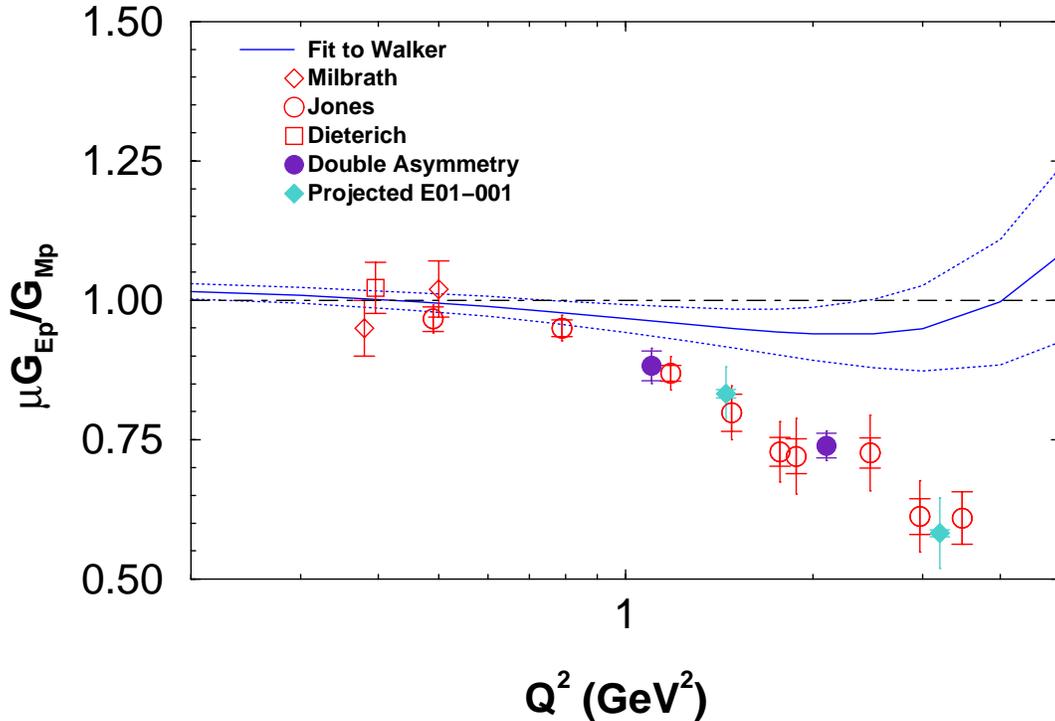


Figure 4: Comparison of projected results from this experiment with the existing Hall A measurements, the approved L-T separation experiment, and a fit to the global analysis of Walker *et al.* with a one sigma error band. The statistical uncertainties are shown with the horizontal bar, while the total uncertainties are shown with the riser only.

L/T results, we offer a very competitive result with a fundamentally different approach than has been performed in the past.

6 Beam Time Requests

A summary of the beam time requested is given in Table 7. In addition to the data collection, we will need to commission the target setup and regularly perform anneals. We assume that the chicane and beamline instrumentation will be commissioned prior to this experiment, so we require only 3 days of commissioning to study the effect of the target field on the SOS and HMS optics. We know from our experience with the target that we will have to anneal the target to restore the polarization about once a day. We assumed 3 hours of annealing

Data Collection	229 h
Anneals	29 h
Commission	72 h
Total	330 h

Table 7: Beam time requests

per day of beam. Moller measurements of the beam polarization can be done during the anneals.

In summary, for 229 hours of data collection we can conduct simultaneous beam-target asymmetry measurements to extract $\mu_p G_{ep}/G_{mp}$ at two Q^2 's. Our approach offers a very competitive means to check the Hall A results against the Rosenbluth separation data in a simple, unassuming manner.

References

- [1] R.C. Walker *et al.*, Phys. Rev. D **49**, 5671 (1994).
- [2] P.E. Bosted, Phys. Rev. C **51**, 409 (1994).
- [3] L. Andivahis *et al.*, Phys. Rev. D **50**, 5491 (1994).
- [4] A.F. Sill *et al.*, Phys. Rev. D **48**, 29 (1993).
- [5] W. Bartel *et al.*, Nucl. Phys. **B58**, 429 (1973).
- [6] L.E. Price *et al.*, Phys. Rev. D **4**, 45 (1971).
- [7] J. Litt *et al.*, Phys. Lett. **31B**, 40 (1970).
- [8] M.N. Rosenbluth, Phys. Rev. **79**, 615 (1950).
- [9] M.K. Jones *et al.*, Phys. Rev. Lett. **84**, 1398 (2000).
- [10] T.W. Donnelly and A.S Raskin, An.. Phys. **169** 247 (1986). T.W. Donnelly and A.S Raskin, An.. Phys. **191** 81 (1989).

[11] R.E. Segel *et al.*, Jefferson Lab Proposal E01-001 (2001).